



1           **Heuristic Approach to Multidimensional Temporal Assignment**  
2           **of Spatial Grid Points for Effective Vegetation Monitoring and Land**  
3           **Use in East Africa**  
4

5                           Virginia M. Miori, Ph.D.<sup>1</sup>, Nicolle Clements, Ph.D.<sup>1</sup>, Brian W. Segulin<sup>2</sup>

6  
7                           <sup>1</sup>Department of Decision and System Sciences, Saint Joseph's University, Philadelphia, PA 19131 USA

8   <sup>2</sup>The Rovisys Company, Aurora, Ohio 44202 USA

9  
10   Correspondence to: Virginia M. Miori ([vmiori@sju.edu](mailto:vmiori@sju.edu))  
11  
12



13 **Abstract:** In this research, vegetation trends are studied to give valuable information toward effective land use in  
14 the East African region, based on the Normalized Difference Vegetation Index (NDVI). Previously, testing  
15 procedures controlling the rate of false discoveries were used to detect areas with significant changes based on  
16 square regions of land. This paper improves the assignment of grid points (pixels) to regions by formulating the  
17 spatial problem as a multidimensional temporal assignment problem. Lagrangian relaxation is applied to the  
18 problem allowing reformulation as a dynamic programming problem. A recursive heuristic approach with a  
19 penalty/reward function for pixel reassignment is proposed. This combined methodology not only controls an  
20 overall measure of combined directional false discoveries and nondirectional false discoveries, but make them as  
21 powerful as possible by adequately capturing spatial dependency present in the data. A larger number of regions are  
22 detected, while maintaining control of the mdFDR under certain assumptions.

23 Data Link: <https://figshare.com/s/ed0ba3a1b24c3cb31ebf>

24 DOI:

25 [https://figshare.com/articles/NDVI\\_and\\_Statistical\\_Data\\_for\\_Generating\\_Homogeneous\\_Land\\_Use\\_Recommendations/5897581](https://figshare.com/articles/NDVI_and_Statistical_Data_for_Generating_Homogeneous_Land_Use_Recommendations/5897581)  
26

27  
28 **Keywords:** Land Use, Mathematical Programming, Dynamic Programming, Multiple Testing, Spatial Data and  
29 Analysis, False Discovery Rate

## 31 1 Introduction

32 Analysis of vegetation life cycles is fundamental in monitoring and planning agricultural endeavors and optimizing  
33 land use. In particular, gaining knowledge of current vegetation trends and using them to make accurate predictions  
34 is essential to minimize times of food scarcity and manage the consumption of natural resources in underdeveloped  
35 countries. Needing to understand the Earth's ecology and land cover is increasingly important as the impacts of  
36 climate change start to affect animal, plant, and human life. Vegetation trends are also closely related to  
37 sustainability issues, such as management of conservation areas and wildlife habitats, precipitation and drought  
38 monitoring, improving land usage for livestock, and finding optimum agriculture seeding and harvest dates for  
39 crops.

40 For this reason, there are many agencies and organizations that focus on the study of land use and land cover trends,  
41 linking them to climate change and the socioeconomic consequences of these changes. The United States Global  
42 Change Research Program (Land Use and Land Cover Change Interagency Working Group), the United Nations  
43 Framework Convention on Climate Change (Land Use, Land Use Change, and Forestry), and NASA's Land Cover  
44 Land Use Change Program are just three examples of well-known interdisciplinary/ interagency programs that  
45 conduct and sponsor research related to the question of global land change as noted in OCHA (2011).

46 Assessment of changes in a region's vegetation structure is challenging, especially in topographically diverse areas,  
47 like East Africa. Forecasting future vegetation and agricultural planning become particularly difficult when



48 unknown trends are occurring. However, the regions with vegetation changes are often the areas of most interest in  
49 land use management. Ideally, an automated screening process can identify areas with significant vegetation  
50 changes and facilitate objective decision making about land-use management such as in Cressie & Wikle (2011).

51 As a first step in creating an automatic screening processes, data collection on vegetation and land cover is needed.  
52 This is typically done through satellite remote sensing. The remote sensing imagery is used to convert the observed  
53 elements (i.e., the image color, texture, tone, and pattern) into numeric quantities at each pixel in the image. The  
54 image pixels correspond to a square grid of land, the size of which depends on the satellite's resolution. One such  
55 numeric indicator is the normalized difference vegetation index (NDVI). In this article, the NDVI series came from  
56 satellite remote sensing data collected between 1982 and 2006 over 8,000-meter grid points. It has been shown to be  
57 highly correlated with vegetation parameters such as green-leaf biomass and green-leaf area, and hence is of  
58 considerable value for vegetation monitoring as in Curran (1980) and Jackson, Et al. (1983).

59 The NDVI standard scale ranges from  $-1$  to  $1$ , indicating how much live green vegetation is contained in the  
60 targeted pixel. An NDVI value close to  $1$  indicates more abundant vegetation. For example, low values of NDVI  
61 (say,  $0.1$  and below) correspond to scarce vegetation consisting mostly of rock, sand and dirt. A range of moderate  
62 values ( $0.2$  to  $0.3$ ) indicates small vegetation such as shrub or grassland; larger NDVI values can be found in  
63 rainforests ( $0.6$  to  $0.8$ ). Often, negative NDVI values are consolidated to be zero since negative values indicate non-  
64 vegetation and are of little use for vegetation monitoring. Vegetation activity is a continuous space-time process and  
65 NDVI data provide a space-time lattice system, in the sense that observations are available over equally spaced  
66 regular grids. Often, the spatial resolution ranges from  $1000$  to  $8000$  meters, while the temporal one ranges from  $7$   
67 days to  $1$  month.

68 Statistical and computational methods are needed to analyze remotely sensed data, like NDVI values, to determine  
69 trends in land condition and to predict areas at risk from degradation. Methodologies that detect land cover changes  
70 need to be sensitive as well as accurate, since it can be costly and risky to relocate human populations, agriculture or  
71 livestock to new regions of detected change. In such spatio-temporal data, time series models are tempting for  
72 representing such processes. Other existing change detection methodologies include the geographically weighted  
73 regression of Foody (2003), the principal component analysis of Hayes & Sader (2001), and the smoothing  
74 polynomial regression of Chen & Tamura (2004). However, these methods are unable to provide an upper bound on  
75 false detections. Since there is large risk associated with falsely declaring an area to have significant vegetation  
76 changes, land use managers seek new methods that have a meaningful control over such errors.

77 In this article, we build on the previous work of Vrieling, et al. (2008) and Clements, et al., (2014). Vrieling, et al.  
78 (2008) first investigated this vegetation screening problem in the hypothesis testing framework of but did not  
79 attempt to address the inherent multiplicity issue by controlling an overall false detection rate while making their  
80 final conclusions. Clements, et. al. (2014) made improvements by incorporating the spatial dependencies, somewhat  
81 arbitrarily, before applying multiple testing procedures. The arbitrary spatial dependency was accounted for by  
82 dividing the region into square blocks, based on an overall measure of spatial correlation using a semivariogram



83 plot. After creating such sub-regions, two-sided monotonic trend tests from Brillinger (1989) were used to identify  
84 significant increasing or decreasing monotonic vegetation changes based on these arbitrarily chosen square regions  
85 of land. They demonstrated that this screening procedure controlled the mixed directional false discovery rate  
86 (mdFDR), which is defined as the expected proportion of Types I errors (False Positives) and Type III errors  
87 (Directional errors) among all rejected null hypotheses, introduced by Benjamini & Yekutieli (2005).

88 In this article, we utilize the same historic NDVI time series for East Africa from 1982 to 2006. Since real-time  
89 monitoring for change is not part of the scope, we focused improving the methodologies previously used to identify  
90 significant changes in land cover in the region. We do this by first framing the research question as an NP-hard  
91 temporal multi-objective assignment problem. Using heuristics to solve this problem, we first find improved sub-  
92 regions than the previous arbitrarily chosen square grids. Using this approach allows us to adequately capture the  
93 specific data structure and answer questions in the present context. Secondly, we reapply the multiple testing  
94 procedures in Clements, et al., (2014) and demonstrate that the testing procedure become more powerful while still  
95 maintaining control an error rate, the mdFDR. In summary, our methods aim to incorporate spatial local  
96 dependencies using a multi-dimensional assignment problem formulation to improve sub-region formation, which in  
97 turn improves the multiple testing results.

98 We organize the paper as follows. In the next section, we give a review of the literature followed by a detailed  
99 description of the historical data set. We then describe the temporal assignment problem formulation to create more  
100 homogeneous sub-regions and explain the heuristic procedure using dynamic programming. Next, we apply the  
101 multiple testing procedures to the improved sub-regions. Finally, we reveal the results of the model implementation,  
102 followed by a discussion, conclusions, and final remarks.

## 103 **2 Literature**

### 104 **2.1 Multiple Testing Overview**

105 To control over false vegetation trend detections, multiple testing procedures can be employed. An overview of  
106 multiple testing notation and procedures are described next. When testing a single null hypothesis against a two-  
107 sided alternative, two types of error can occur when a directional decision is made following rejection of the null  
108 hypothesis. These are Type I error and Type III (or directional) errors. The Type I error occurs when the null  
109 hypothesis is falsely rejected, while the Type III error occurs when the null hypothesis is correctly rejected but a  
110 wrong directional decision is made about the alternative.

111 Consider testing  $n$  hypotheses simultaneously, such as testing for trend changes in  $n$  pixels over the East African  
112 region. Table 1 gives the various outcomes of these tests, where  $H_{i0}: \theta_i = \theta_{i0}$  is the null hypothesis and  $H_{i1}: \theta_i \neq$   
113  $\theta_{i0}$  is the two-sided alternative, for  $i = 1, 2, \dots, n$ . Of these quantities in Table 1, only  $n, A$ , and  $R$  (where  $R = R_1 +$   
114  $R_2$ ) are known after applying a particular testing procedure. The number of Type I errors, Type II errors, and Type  
115 III errors are  $V = V_1 + V_2$ ,  $T = T_1 + T_2$ , and  $U = S_2 + S_3$  respectively. All three quantities are unknown but



116 desirably small. Most multiple testing procedures focus on controlling  $V$  in some capacity. In this paper, we utilize a  
 117 procedure that controls  $V$  and  $U$ .

		Decision			Total
		Fail to Reject Null	Reject Null $H_0^{(+)}$	Reject Null $H_0^{(-)}$	
Truth	$\theta = \theta_0$	$W$ (Correct Decisions)	$V_1$ (Type I errors)	$V_2$ (Type I errors)	$n_0$
	$\theta > \theta_0$	$T_1$ (Type II errors)	$S_1$ (Correct Decisions)	$S_2$ (Correct Decisions)	$n_+$
	$\theta < \theta_0$	$T_2$ (Type II errors)	$S_3$ (Correct Decisions)	$S_4$ (Correct Decisions)	$n_-$
Total		$A$	$R_1$	$R_2$	$n$

118

119

**Table 1: Multiple Testing outcomes from testing  $n$  hypotheses**

120 One of the most commonly used measures of overall Type I error is called the Familywise Error Rate (FWER). The  
 121 FWER is the probability of making one or more Type I errors. In other words, out of  $n$  simultaneously tested  
 122 hypotheses, where  $V$  is the number of Type I errors made out of  $n$  decisions (recall:  $V$  is an unknown quantity), then  
 123  $\text{FWER} = \text{Prob}\{V > 0\}$ . In the case of multiple hypothesis testing, the FWER should be controlled at a desired  
 124 overall level, called  $\alpha$ . The Bonferroni procedure is the most popular method to control the FWER, but there are  
 125 other techniques, such as those in Holland & Copenhaver (1987), Hochberg & Tamhane (1987), Šidák (1967), Holm  
 126 (1979), Hochberg (1988), Sarkar (1998), and Sarkar & Chang (1997).

127 The False Discovery Rate (FDR), proposed by Benjamini and Hochberg (1995), is the second most common  
 128 measure of Type I errors. The FDR is the expected proportion of Type I errors among all the rejected null  
 129 hypotheses. If there are no rejected hypotheses, the FDR is defined to be zero. In terms of Table 1,  $\text{FDR} =$   
 130  $E\left[\frac{V}{\max(R, 1)}\right]$ . Comparatively, the FDR is less conservative than the FWER, meaning FWER control ensures  
 131 FDR control. However, a multiple testing procedure with FDR control will not necessarily maintain control of the  
 132 FWER. The FDR is a widely accepted and utilized notion of Type I errors in large-scale multiple testing  
 133 investigations. Recent literature has proposed methods to control the FDR, including Benjamini and Hochberg  
 134 (1995), Benjamini and Yekutieli (2001), Sarkar (2002), Blanchard and Roquain (2009), Storey, Taylor, and  
 135 Siegmund (2004), and Benjamini, Krieger, and Yekutieli (2006).

136 Often, it becomes essential for researchers to determine the direction of significance, rather than significance alone,  
 137 when testing multiple null hypotheses against two-sided alternatives. In other words, for each test, researchers have  
 138 to decide whether or not the null hypothesis should be rejected and, if rejected, determine the direction of the  
 139 alternative. Typically, this direction is determined based on the test statistic falling in the right- or left-side of the  
 140 rejection region. Such decisions can potentially lead to one of two types of error for each test resulting in rejection of  
 141 the null hypothesis - the Type I error if the null hypothesis is true or the directional error, also known as the Type III



142 error, if the null hypothesis is not true but the direction of the alternative is falsely declared (i.e. a rejection of a false  
143 null using a two-sided alternative, but where the sign of the true parameter, say  $\beta_i$ , is opposite of its estimate  $\hat{\beta}_i$ ).

144 Two variants to deal with Type I and Type III errors have been introduced in the literature. First is the pure  
145 directional FDR (dFDR), which is the expected proportion of directional errors among rejected hypotheses. Second  
146 is the mixed directional FDR (mdFDR), which is the expected proportion of Type I and Type III errors among  
147 rejected hypotheses. To deal with both errors in an FDR framework, the notion of mixed directional FDR (mdFDR)  
148 was been introduced by Benjamini et al. (1993). Since then, other methods to control directional errors have been  
149 introduced, including Benjamini and Yekutieli (2005), Benjamini and Hochberg (2000), Shaffer (2002), Williams et  
150 al. (1999), Guo et al. (2009), and Sarkar and Zhou (2008).

151 Controlling both false discoveries ( $V$ , from Table 1) and directional false discoveries ( $U$ , from Table 1) is important  
152 in this application. For instance, when declaring a particular  $8,000 \text{ m} \times 8,000 \text{ m}$  grid of land as ‘significantly’  
153 changing in terms of vegetation, a Type I error is made if the area is not truly changing, and a Type III error is made  
154 if the area is truly changing but in the opposite direction of what is determined from the data. When such decisions  
155 are made simultaneously based on testing multiple hypotheses, one should adjust for multiplicity and control an  
156 overall measure of Types I and III errors. Without such multiplicity adjustment, more Types I and III errors can  
157 occur than the desired  $\alpha$  level. It is particularly important to avoid these errors as much as possible in the present  
158 application. Land use managers, government and local farmers are looking to relocate East African populations of  
159 people, livestock and crops to areas of promising vegetation changes and avoid regions with decreasing changes.  
160 Since these migrations can be risky and costly, a careful consideration of the multiplicity issue seems essential when  
161 making declarations of significant vegetation changes.

162 In this article, p-values generated using the monotonic trend test in Brillinger (1989) are computed for each site  
163 ( $8,000 \text{ m} \times 8,000 \text{ m}$  grid of land) and provide evidence of vegetation change occurring over the years—the smaller  
164 the p-value, the higher is the evidence of a significant vegetation change. For each site, a decision must be made  
165 regarding the significance of vegetation change that might have occurred over the years at that site, and, if  
166 vegetation change is found significant, determine the direction in which this change has taken place. This must be  
167 done simultaneously for all sites ( $\approx 50,000$ ) in the East African region in a multiple testing framework designed to  
168 ensure a control over a meaningful combined measure of statistical Types I and III errors.

169 In this paper, we will first be framing the research question as a heuristic multi-objective temporal assignment  
170 problem, in which better sub-regions were created than the arbitrarily chosen square grids in Clements et.al. (2014).  
171 By using temporal assignments to create subregions, we will demonstrate that the testing procedure becomes more  
172 powerful. Also in this article, we provide theoretical proof that the mdFDR is still controlled under sub-region  
173 independence.

## 174 **2.1 Temporal Assignment Problem Overview**



175 There is a wealth of research on assignment problems and specialized assignment problems that display  
176 complicating constraints. Though the generalized assignment problem is solvable, once the number of dimensions  
177 reaches 3, as in the formulation presented in this paper, this is no longer the case.

178 The multidimensional assignment problem was introduced by Pierskalla (1968) and a bibliography of multidimensional assignment problems was prepared by Gilbert & Hofstra (1988). Miori (2011, 2008, 2014) used  
179 assignment problems to model truckload routing problems and the Pollyanna gift exchange problem. Scheduling  
180 medical residents with the temporal component was addressed by Franz & Miller (1993). Bandelt, Et al. (1994,  
181 2004) addressed multi-dimensional assignment problems with decomposable costs. The three-dimensional  
182 assignment problem was applied to teaching schedules by Frieze & Yadegar (1981) and Balas & Saltman (1991).  
183 Multidimensional approximation was applied to capacity expansion problems by Troung & Roundy (2011).  
184 Lagrangian Relaxation was applied to a multi-dimensional assignment problem arising from multi-target tracking by  
185 Poore & Rijavec (1993). Multi-tracking data was also addressed by Robertson (2001).  
186

187 Approximations to the multi-dimensional assignment problem were generated by Kuroki & Matsui (2007), Gutin,  
188 Et al. (2008), Krokhmal, Et al. (2007), and Karapetyan & Gutin (2011). The multi-objective assignment problem  
189 seeking solutions to the assignment problem in the face of additional objectives using efficient sets was posed by  
190 White (1984). A weighting function approach has also been applied to multi-objective (multicriteria) problems with  
191 conflicting objectives by Phillips (1987).

192 Agricultural planning problems have been addressed by Samuelson (1952), Takayama (1964), Norton & Scandizzo  
193 (1981), Kutcher & Norton (1982), Önal & McCarl, and Weintraub & Romero (2017). Multicriteria approaches to  
194 agriculture decisions have also been applied by Gasson (1973), Harper & Eastman (1980), Wheeler & Russel  
195 (1977), Hayashi (2000), and Romero & Rehman (2003).

196

## 197 **2.2 Land Use Optimization Overview**

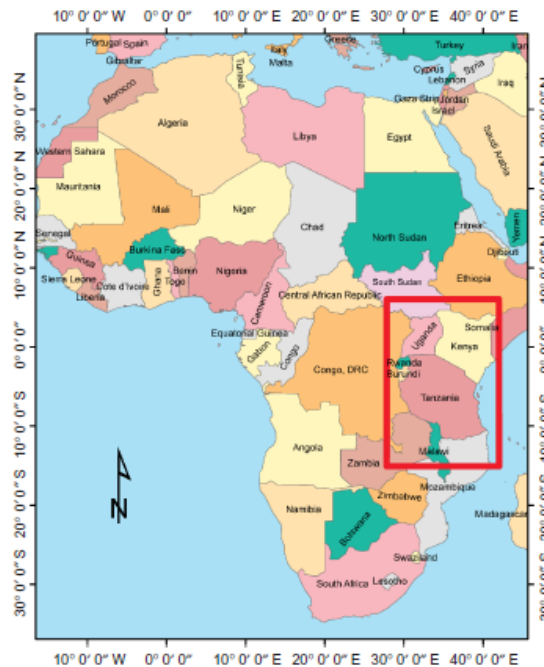
198 The most basic methods in land use optimization involve limited enumeration of alternatives and developing metrics  
199 to directly assess these alternatives. Landscape metrics addressing various land use goals were used by Kuchma, Et  
200 al. (2013) to evaluate enumerated options for land use. A similar approach was proposed by Wang & Guldman  
201 (2015) to mitigate seismic damages in Taichung, Taiwan.

202 Heuristic methods and in sustainable land use were applied by Steward, Et al. (2004), Cao, Et al. (2011), Liu, Et al.  
203 (2016) and Sahebgharani (2016). Genetic algorithms were presented Cao, Et al. (2012) and the Analytical  
204 Hierararchy Process was utilized by Memarian, Et al. (2014). Multi-objective linear programming with sensitivity  
205 analysis was found effective by Sadeghi, Et al. (2009) while Soil and Water Assessment Toll (SWAT) was  
206 employed by Sunandar, Et al. (2014).



### 207 3 Data Description

208 East Africa spans a wide variety of climate types and precipitation regimes which are reflected in its vegetation  
209 cover. To capture this, satellite imagery was collected over a sub-Saharan region of East Africa that includes five  
210 countries in their entirety (Kenya, Uganda, Tanzania, Burundi and Rwanda) and portions of seven countries  
211 (Somalia, Ethiopia, South Sudan, Democratic Republic of Congo, Malawi, Mozambique and Zimbabwe). This  
212 roughly ‘rectangular’ region extends from 27.8°E to 42.0°E longitude and 15.0°S to 6.2°N latitude. Also included in  
213 the region are several East African Great Lakes such as Lake Victoria, Lake Malawi and Lake Tanganyika.  
214 Vegetative analysis in this region is of interest for a variety of reasons, including the importance of the region for  
215 global biodiversity and the vulnerability of the region to climate change, deforestation of the Congo, urban  
216 development, civil conflict, and agricultural practices.



217

218

219

Figure 1 The study area, as indicated by the box.

220 The remotely sensed images were recorded twice a month from 1982–2006 and then converted to NDVI values.  
221 Hence, the spatio-temporal data set consists of approximately 50,000 sites (pixels), each with 600 time series  
222 observations (24 observations per year over 25 years). The satellite’s resolution corresponds to each pixel spanning  
223 an 8,000m × 8,000m grid of land, which we will refer to as a ‘location.’ This Global Inventory Modeling and  
224 Mapping Studies (GIMMS) data set is derived from imagery obtained from the Advanced Very High Resolution



225 Radiometer (AVHRR) instrument onboard the National Oceanic and Atmospheric Administration (NOAA) satellite  
226 series 7, 9, 11, 14, 16 and 17. The NDVI values have been corrected by Tucker, Et al. (2005) for calibration, view  
227 geometry, volcanic aerosols, cloud coverage and other effects not related to vegetation change.

228 All the negative NDVI values were consolidated to zero, as commonly done in vegetation monitoring, and re-scaled  
229 the remaining values by 1,000. Negative NDVI values indicate non-vegetation areas, and so they are of no use in our  
230 statistical analysis. Prior to the analysis, we examined the data for quality assurance and eliminated a small number  
231 of pixels that were found to have several consecutive years with identical data values, which may be due to data  
232 entry errors or machine malfunction.

233 When this data was first examined in Vrieling, de Beurs and Brown (2008), the percentage of pixels with the trend  
234 test p-value less than  $\alpha = 0.10$  was reported separately for positive and negative slopes. The reported results indicate  
235 that much of the region has ‘significant’ vegetation change. For example, the cumulative NDVI indicator detected  
236 44.2% of sites with p-values less than 0.10. However, this result fails to address the important statistical issue of  
237 multiplicity when making these claims about significant vegetation changes and their directions simultaneously for  
238 all the regions based on hypothesis testing. Later, Clements, et. al. (2014) addressed the multiplicity issue by  
239 proposing a 3-stage multiple testing procedure to control the mixed-directional False Discovery Rate (mdFDR), but  
240 did so on subregions of East Africa that were not optimally formed.

241 The associated csv file for this analysis is the information generated from Clements, et al, (2014) which was the  
242 initial starting point for this analysis. It contains the following fields:

- 243 • site: Consecutive ID number, acting as a unique identified
- 244 • xcoord: pixel longitude
- 245 • ycoord: pixel latitude
- 246 • ndvi.avg: Overall pixel average NDVI from 1982 to 2006 (observations taken twice monthly)
- 247 • pval: Resulting p value from the Brillinger Trend Test (Brillinger, 1989)
- 248 • slp: Resulting slope from the Brillinger Tren Test (Brillinger, 1989)
- 249 • block: Block number – initial assignment was arbitrary

250 Using the algorithm below, followed by the multiple testing procedure, users may generate the revised and improved  
251 block assignments.

252

#### 253 **4 Assignment Problem Formulation**

254 We propose an assignment formulation to this problem, using these analysis results, with the goal of an improved  
255 solution. The object of the geographic assignment problem is to map each pixel within the satellite images to an  
256 appropriate block based upon a target value for each block. The block target values represent equal size ranges  
257 within the overall range of the objective function values. The objective function for the pixel assignment is the sum



258 of absolute difference between the pixel NDVI and the block target NDVI. The number of blocks is set objectively  
 259 and may be reset for each assignment problem solution generated.

260 Note that pixels may be formed entirely of water; these pixels have been assigned arbitrarily high NDVI values to  
 261 effectively eliminate them from consideration in the block assignments. A ‘water block’ with an arbitrarily high  
 262 target value ensures that all of these pixels may be assigned to blocks.

263 The objective of the pixel assignment problem is to minimize the NDVI difference function. Let  $m$  = the number of  
 264 pixels, let  $n$  = the number of blocks, and let  $T$  = the number of time periods. The decision variable  $x_{ij}^k$  is a binary  
 265 variable that represents the assignment, or lack of assignment, of pixel  $i$  to block  $j$  at time  $k$ . The constraints  
 266 formulated ensure that each pixel is assigned to a block, during each period of time. The formulation in Eq. (1) – (3)  
 267 follows the notation.

$x_{i,j}^k$	Decision variable $\in (0,1)$ $i = 1, \dots, m; j = 1, \dots, n; k = 1, \dots, T$
$N_i^k$	Pixel $i$ NDVI score for time $k$ : $i = 1, \dots, m; k = 1, \dots, T$
$N_j^k$	Block $j$ NDVI target for time $k$ : $j = 1, \dots, n; k = 1, \dots, T$

268 **Table 2 Assignment Problem Notation.**

269

270 
$$\text{Minimize } \sum_k \sum_j \sum_i |N_j^k - N_i^k| \cdot x_{i,j}^k \quad (1)$$

271 Subject to:

272 
$$\sum_i \sum_j x_{i,j}^k = 1 \text{ for } k = 1, \dots, T \quad (2)$$

273 
$$x_{i,j}^k \in (0,1) \quad (3)$$

274 The binary decision variables utilize three indices, rendering the problem NP hard. We therefore propose and  
 275 employ a heuristic approach that relies heavily on dynamic programming.

276 **5 Assignment Problem Solutions**

277 **5.1 Lagrangian Relation**

278 Restatement of the pixel assignment problem as a Markov Process will facilitate alternative solution methodologies.  
 279 We present a Lagrangian relaxation of the formulation and introduce a Lagrangian multiplier ( $\varphi_k$ ) for the single  
 280 constraint to be relaxed in each time period  $k = 1, \dots, T$ . We include a simplifying assumption that the penalty is  
 281 constant over all time periods and is denoted as  $\varphi$ . The revised formulation is presented in Eq. (4) - (5).



282

$$\text{Minimize } \sum_k \sum_j \sum_i |N_j^k - N_i^k| \cdot x_{i,j}^k + \sum_k \varphi \left( \sum_j \sum_i x_{i,j}^k - 1 \right) \quad (4)$$

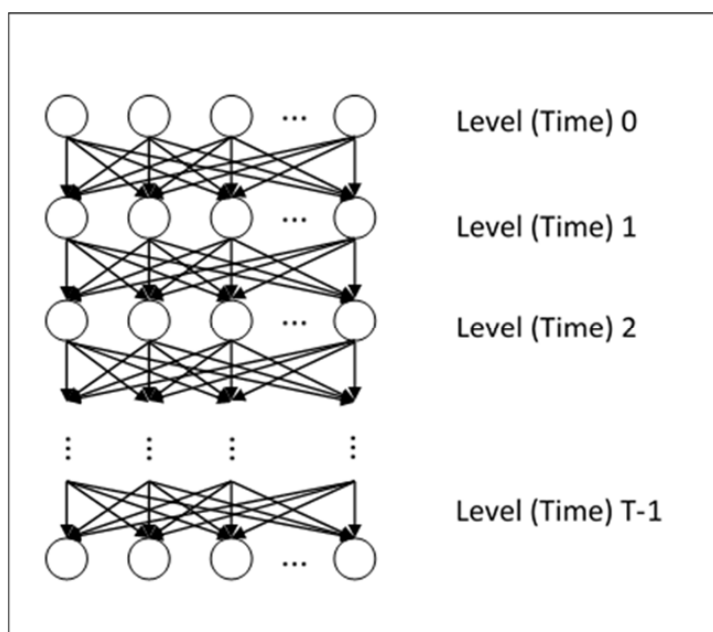
283 Subject to:

$$284 \quad x_{i,j}^k \in (0,1) \quad (5)$$

285 A dynamic programming formulation may now be presented using the relaxed formulation.

286 **5.2 Dynamic Programming Formulation**

287 The pixel assignment decisions may be made in stages, and while the outcome of each decision is not fully  
 288 predictable, it can be observed before the next decision is made. We begin the dynamic programming formulation  
 289 by organizing the problem into a tree structure (Fig. 2) reflecting pixels and levels (time increments). Each level of  
 290 the tree corresponds to a time increment, beginning with time 0 which represents the first satellite images retrieved  
 291 within the data set and ending at the final images at time T-1 and the pixels in each level number from 1 to m. The  
 292 tree provides a discrete-time dynamic system.



293

294

295

Figure 2 General Tree Structure.



296 An additive value function reflects both present cost of each pixel assignment to a block, and potential future cost of  
 297 all pixel assignments to blocks (expected cost-to-go). Block NDVI targets must be established in order to match  
 298 pixels to blocks. Initialization of these targets is accomplished by evenly distributing the range of NDVI values  
 299 across  $n$  candidate blocks. Recall that the NDVI values ranges between 0 and 1000, resulting in block targets  
 300 starting at zero with an increment  $1000/n$  up to 1000.

301 To calculate expected cost-to-go, we must also identify and calculate transition probabilities. In doing so, we  
 302 consider only the current level (time period). The Markov Property (6) allows us to omit consideration of the  
 303 probabilities of the path leading to the current level. The tree may now be viewed as a finite Nonhomogeneous  
 304 Markov Process with transition probability matrix  $P^{(k)}$  representing transitions at any level.

$$305 \quad P(X_{k+1} = x_{k+1} | X_0 = x_0, \dots, X_k = x_k) = P(X_{k+1} = x_{k+1} | X_k = x_k) \quad (6)$$

306 The objective of the dynamic programming formulation is the minimization of the sum of cost at the current stage,  
 307 and the cost-to-go (the best case to be expected from future stages). The notation required for the formulation  
 308 follows.

$A(k+1, k)$	Available pixels at level (time) $k+1$ , depends on pixel chosen at level $k$
$m_{k+1}$	Cardinality of $A(k+1, k)$ (the number of pixels available at level $k+1$ , depends on pixel selected at level $k$ )
$s(k)$	The pixel chosen at level $k$
$P^{(k)}$	Transition probability matrix at level $k$
$P_{i,j}^{(k)}$	Transition probability of moving from pixel $i$ to pixel $j$ at level $k$
$C_{s(k),j}$	Cost of adding node $j$ after the pixel chosen at level $k$
$U(i, k)$	The number of unassigned pixels if we choose pixel $i$ at level $k$
$f(i, k)$	Expected cost-to-go if we choose pixel $i$ at level $k$
$f(1,0)$	Initialize to 0
$\varphi$	Pixel assignment penalty

309

310 Pixel assignments to blocks may begin at any pixel in level 0 of the tree and end at any pixel in level  $T-1$ . All pixels  
 311 must be assigned to a single block but individual blocks need not have pixels assigned to them. Let  $z$  be the  
 312 candidate block.

$$313 \quad f(s(k), k) = \min_{z \in A(k+1, k), \varphi} \left\{ C_{s(k),z}^k + P_{i,j}^{(k)} \varphi U(s(k), k) + f(z, k+1) \right\} \quad (7)$$

$$314 \quad C_{s(k),z}^k = |N_z^k - N_{s(k)}^k| \quad (8)$$

315 Though this approach resolves issues with the original assignment formulation, it necessitates the calculation of  
 316 transition probability matrices ( $P^{(k)}$ ) at each level. Transition probabilities are dependent on the number of blocks  
 317 chosen, and the ability to statistically characterize the changes in vegetation in the pixels over time. With as few as



318 100 blocks, the probabilities would have a very small order of magnitude and an expectation of high levels of  
 319 inaccuracy, resulting in a lack of ability to detect meaningful differences. We present a heuristic, rooted in dynamic  
 320 programming principles to render an efficient and useful solution to the pixel assignment problem.

### 321 5.3 Recursive Heuristic Procedure

322 Due to the original assignment problem being NP hard, and the dynamic programming approach resulting in  
 323 extreme computational and structural complexity, we introduce a heuristic method that leverages knowledge gained  
 324 in the assignment and dynamic programming approaches. This heuristic also leverages the previous research  
 325 completed in controlling the mdFDR.

326 The heuristic procedure was initialized with the 150 blocks used in Clements et. al (2014) and 56,355 total pixels,  
 327 and utilized the previously calculated slopes and resulting p-values from monotonic trend tests. Rather than  
 328 assigning the pixels to blocks over the duration of the 25-year span of the data collection as the assignment  
 329 formulation would, this approach focused on assignment at the final observations in the 25th year but the use of  
 330 slope and p-value allowed the approach to reflect the trends that occurred over time. This same approach could be  
 331 used at any time during the study, reflecting all previous data.

332 The heuristic performance metric, like the objective function in the pixel assignment problem, required the  
 333 calculation of block values corresponding to the pixel values. The metric leverages the initial random blocks by  
 334 including the block average NDVI, the block average slope, the block average p-value, and the slope change  
 335 indicator variable. Notation is introduced in Table 3, followed by the formulation of the performance metric.

$y_{fg}$	Block assignment $\in (0,1)$ $f = 1, \dots, m; g = 1, \dots, n$
$I_{fg}$	Slope change Indicator variable
$N_f$	Pixel $i$ NDVI score at final observation: $i = 1, \dots, m$
$NR_g$	NDVI range for block $g$
$S_f$	Pixel $i$ slope over time: $i = 1, \dots, m$
$SR_g$	Slope Range for block $g$
$P_f$	Pixel $i$ p-value over time: $i = 1, \dots, m$
$PR_g$	p-value range for block $g$
$w_d$	Weight for scoring factor $d$ : $d = 1, \dots, 4$

336 **Table 3 Heuristic Metric Notation.**

337 Let  $f$  = pixel number and let  $g$  = block number and let

$$338 y_{fg} = \begin{cases} 1 & \text{if pixel } f \text{ is assigned to block } g \\ 0 & \text{if pixel } f \text{ is not assigned to block } g. \end{cases}$$

339



340 Development of the performance metric required definition of the block average values for NDVI, slope and p-value  
 341 shown in Eq (9) – (11). In addition, the indicator parameter, signaling slopes of opposite sign is shown in Eq. (12).

$$342 \quad \bar{N}_{.g} = \sum_{f \ni \text{pixels} \in \text{block } g} \frac{N_{fg}}{n} \quad \forall g = 1, \dots, n \quad (9)$$

$$343 \quad \bar{S}_{.g} = \sum_{f \ni \text{pixels} \in \text{block } g} \frac{S_{fg}}{n} \quad \forall g = 1, \dots, n \quad (10)$$

$$344 \quad \bar{P}_{.g} = \sum_{f \ni \text{pixels} \in \text{block } g} \frac{P_{fg}}{n} \quad \forall g = 1, \dots, n \quad (11)$$

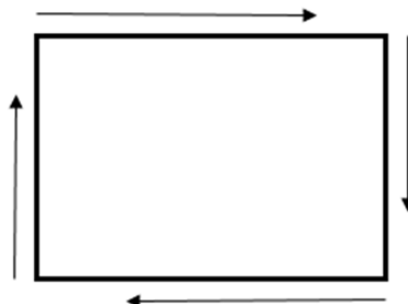
$$345 \quad I_{fg} = \begin{cases} 1 & \text{if } \text{sign}(S_f \cdot \bar{S}_{.g}) \text{ is negative } \forall f \ni \text{pixels} \in \text{block } g \\ 0 & \text{if } \text{sign}(S_f \cdot \bar{S}_{.g}) \text{ is positive } \forall f \ni \text{pixels} \in \text{block } g \end{cases} \quad (12)$$

346 The minimum value of the performance metric in Eq. (13) determines the highest quality heuristic solution. Pixels  
 347 whose current assignment leaves them on the border between blocks are evaluated. The metric is calculated for their  
 348 incumbent (current) assignment and their prospective assignment(s). The pixel is then assigned to the block yielding  
 349 the lowest value of the metric. As pixels are reassigned, newly exposed border pixels are evaluated in the same  
 350 fashion. This procedure continues until all border pixels belong to the block with the best fit.

$$351 \quad w_1 \frac{|N_f - \bar{N}_{.g}|}{NR_g} + w_2 \frac{|S_f - \bar{S}_{.g}|}{SR_g} + w_3 \frac{|P_f - \bar{P}_{.g}|}{PR_g} + w_4 I_{fg}$$

$$352 \quad \forall \text{ pixel } f = 1, \dots, m; \text{ bordering block } g = 1, \dots, n \quad (13)$$

353 The dynamic programming concept of forward and backward passes has been adapted for the heuristic to  
 354 compensate for directional bias in the results. In this way, all border pixel assignments may be evaluated in all  
 355 directions. Four starting points and starting directions are identified in Fig. 3. Fig. 4 shows the four passes to be  
 356 completed for the first starting direction (upper left-hand corner). The first two passes are the forward direction  
 357 evaluation and the second two passes are the backward direction evaluation. These same four passes are adapted for  
 358 each starting point/direction, with the first pass always corresponding to the starting position.

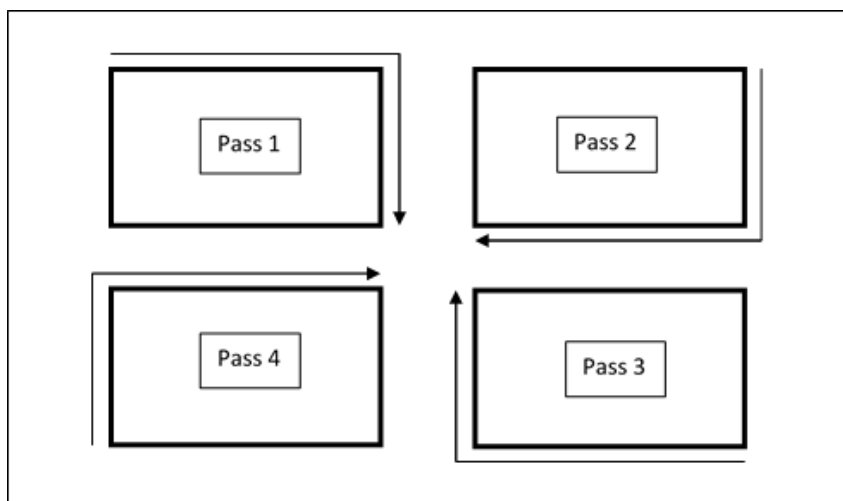


359



360  
361

Figure 3 Starting Directions for Evaluation of Pixel Assignments.



362

Figure 4 Forward-backward evaluation: Forward passes 1 and 2; Backward passes 3 and 4.

363

364

365 Implementation and validation of the heuristic was accomplished through the development of a program written in  
366 the C programming language.

## 367 6 Reassignment Model and Implementation

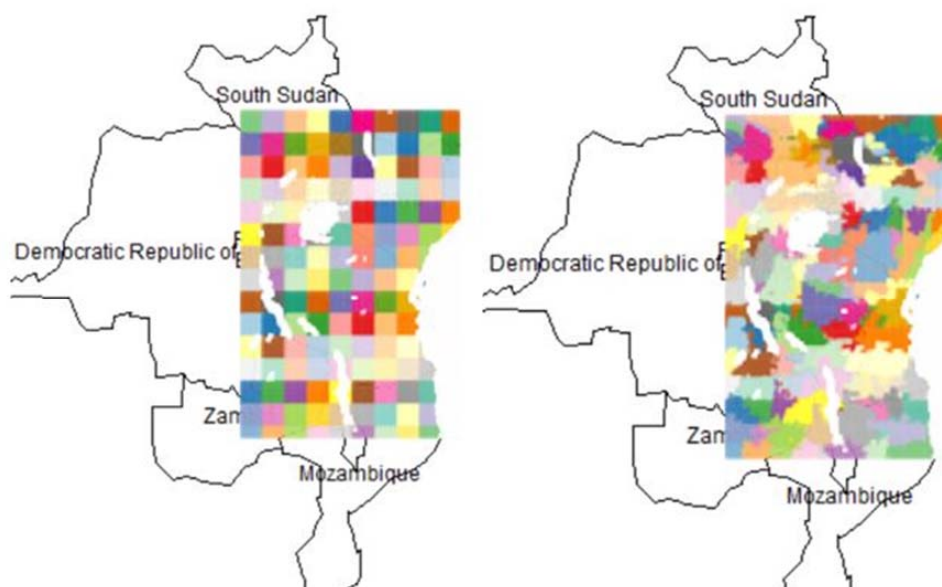
368 An approach inspired by dynamic programming was utilized to find the best solution to the heuristic problem based  
369 on weight factors that varied between 0 to 1, under the condition that  $\sum_{i=1}^4 w_i = 1$ . Table 4 shows a subset of the  
370 factor weight combinations that were examined. As seen in Table 4, selecting the solution with factor scores of  
371  $w_1 = 1$ ,  $w_2 = 0$ ,  $w_3 = 0$ , and  $w_4 = 0$  generates the smallest value of the performance metric in Eq. (13). Since  
372 factor 1 represents the NDVI average value at the final observation, this solution suggests performing pixel  
373 reassignment based solely on NDVI information with no weight applied to factors such as slope and p-value. The  
374 average score function of initial arbitrary square grid solution (calculated to be 0.1339) was compared to the  
375 proposed reassignment solution (calculated to be 0.0998), and yielded an improvement of 25.5%.

376 [Table 4 near here]

377 The spatial map in Fig. 5 visualizes the initial arbitrary block assignment using square grids (left) compared to the  
378 final solution (right) that gave the minimum value of the performance metric in Eq. (13). The contrast in maps  
379 reveals how the solution to the pixel assignment problem created natural looking clusters of differing sizes. For  
380 example, along some coastline areas, clusters are long and narrow. This is intuitive because NDVI values tend to be



381 similar along the coast where many areas are comprised of sand and rock. In other areas, clusters became circular  
382 and cover vast areas of known deserts in the East African regions. Small clusters also exist in the solution and, after  
383 investigating, we found that many of these clusters comprise of cities and urban areas that have little vegetation. It  
384 is logical that such pixels should be reassigned into the same cluster.



385

386 Figure 5 Initial arbitrary block assignment (left) compared to final solution (right).

387

388 An unbiased validation of the reassignment solution can be calculated using the average coefficient of variation for  
389 the final pixel assignment and compare it to the initial square block assignment. The coefficient of variation (CV) is  
390 a unit-less measure of spread that describes the amount of variability relative to the mean. CV is defined as the ratio  
391 of standard deviation over the mean. Smaller values of CV indicate higher homogeneity of the clusters. The  
392 average of cluster's coefficients of variations for our final pixel assignment solution is 11.762. This is a 27.4%  
393 decrease compared to the average coefficient of variation for the original square blocks, which was 16.205. This is a  
394 statistically significant difference in CV averages ( $p=0.000529$ ), providing further evidence that the pixel  
395 reassignment solution was able to increase the level of homogeneity within clusters. Having homogeneous clusters  
396 is important when making large scale decisions about regions in East Africa that have experienced significant  
397 vegetation trend changes.

## 398 7 Multiple Testing Implementation and Results



399 Now we can assume that the pixels in the East African region are divided into homogeneous subregions using  
 400 temporal assignments, as described above. Next, we summarize and apply the multiple testing procedure given in  
 401 Clements, et. al. (2014).

402 For notation, let  $m$  be the number of such subregions and  $n_i$  be the number of pixels/locations in the  $i^{\text{th}}$  subregion.  
 403 P-values at each location were calculated using a two-sided monotonic trend test at each location using the Brillinger  
 404 (1989) test. Specifically, we denote  $\beta_{ij}$  as the monotonic trend parameter as defined in the Brillinger test for the  $i^{\text{th}}$   
 405 subregion and  $j^{\text{th}}$  location, where  $i = 1, 2, \dots, m$ ,  $j = 1, 2, \dots, n_i$ . We also let  $T_{ij}$  and  $P_{ij}$  be, respectively, the test  
 406 statistic and the corresponding p-value for testing the null hypothesis  $H_{ij}: \beta_{ij} = 0$  against its two-sided alternative  
 407  $H_{i1}: \beta_{ij} \neq 0$ .

408 We apply Clements, et. al. (2014) suggestion of using a Bonferroni correction at each subregion, which combines  
 409 the p-values by calculating  $P_i = n_i \min_{1 \leq j \leq n_i} (P_{ij})$ . With  $H_{ij}$  representing the null hypothesis corresponding to  $P_{ij}$ ,  
 410 consider  $H_i = \bigcap_{j=1}^{n_i} H_{ij}$  as the null hypothesis corresponding to  $i^{\text{th}}$  subregion. We will test the  $H_{ij}$ 's against their  
 411 respective two-sided alternatives and detect the direction of the alternatives for the rejected hypotheses.  
 412 Specifically, we apply the procedure using  $\alpha=0.05$  in the following three steps:

413 *Multiple Testing Procedure Applied to Homogeneous Sub-regions:*

414 1) Apply the BH method to test  $H_i$ ,  $i = 1, 2, \dots, m$ , based on their respective p-values  $P_1, P_2, \dots, P_m$  as follows:  
 415 consider the increasingly ordered versions of the  $P_i$ 's,  $P_{(1)} \leq P_{(2)} \leq \dots \leq P_{(m)}$ . Find  $S = \max\{i: P_{(i)} \leq i\alpha/m\}$ .  
 416 Reject the  $H_i$ 's for which the p-values are less than or equal to  $P_{(S)}$ , provided this maximum exists, otherwise, accept  
 417 all  $H_i$ .

418 2) For every  $i$  such that  $H_i$  is rejected at step 1, consider testing  $H_{ij}$ ,  $j = 1, 2, \dots, n_i$  based on their respective p-  
 419 values  $P_{ij}$ ,  $j = 1, 2, \dots, n_i$ , as follows: reject  $H_{ij}$  if  $P_{ij} \leq S\alpha/mn_i$ .

420 3) For each rejected  $H_{ij}$  in step 2, decide the direction of the monotonic trend to be the same as that of  
 421  $\text{sign}(T_{ij})$ .

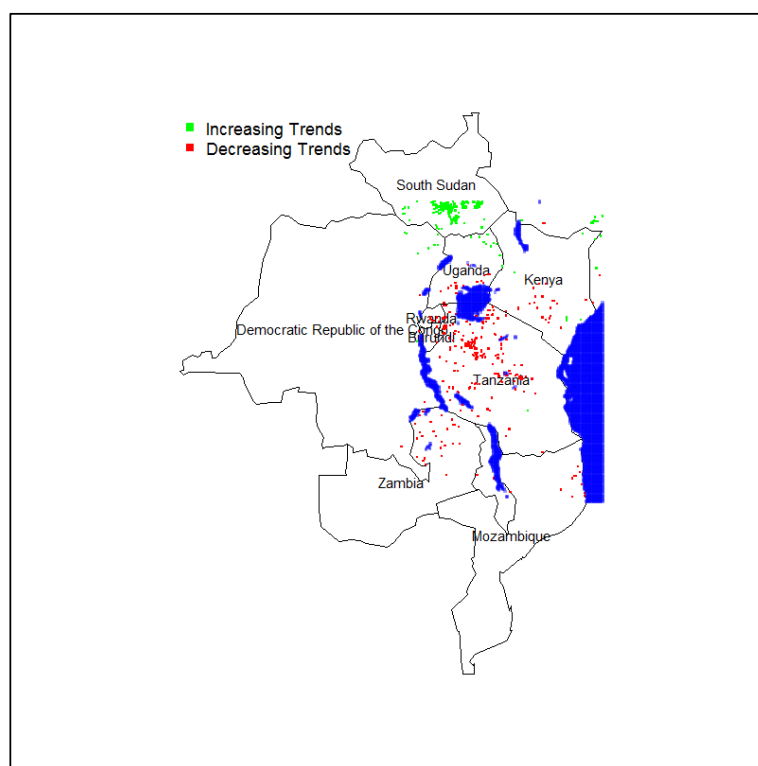
422 Step 1 and 2 identify first, the subregions and second, the locations with significant vegetation changes. The third  
 423 step allows one to make a more detailed analysis by identifying the directions in which these significant changes  
 424 have occurred. Impressively, this procedure controls the mdFDR at level  $\alpha$  if the subregions are independent. A  
 425 mathematical proof of this is given in the Appendix.

426 The results of implementing this procedure to our homogenous subregions are shown in Fig. 6. Sites with a  
 427 significant increasing change in vegetation are plotted in green. Sites with significant negative vegetation change are  
 428 plotted in red. The nonsignificant sites are represented by white. Using the temporal reassignment to form



429 homogeneous subregions before implementing the multiple testing procedure detected 518 locations with significant  
 430 vegetation changes. Compared to the procedure in Clements, et. al. (2014) based on arbitrary square subregions,  
 431 this is an increase in 10 detected locations, which is indicative of a higher-powered testing procedure, while still  
 432 maintaining control over Type I and Type III errors.

433 Geographically, the results show increasing vegetation trends in the Northern hemisphere as well as coastal Eastern  
 434 Tanzania. Decreasing vegetation trends are mostly concentrated directly South of Lake Victoria. These findings are  
 435 consistent with historical evidence and other climate change investigations done in this region.



436

437 Figure 6 Pixels detected using the proposed heuristic reassignment solution with multiple testing procedures.

438 **8 Data Availability**

439 The data, titled "NDVI and Statistical Data for Generating Homogeneous Land Use Recommendations", may be  
 440 accessed through figshare. The link to the archives is: <https://figshare.com/s/ed0ba3a1b24c3cb31ebf> and the DOI is  
 441 [https://figshare.com/articles/NDVI\\_and\\_Statistical\\_Data\\_for\\_Generating\\_Homogeneous\\_Land\\_Use\\_Recommendations/5897581](https://figshare.com/articles/NDVI_and_Statistical_Data_for_Generating_Homogeneous_Land_Use_Recommendations/5897581).  
 442

443 **9 Conclusions and Future Research**



444 It is important to consider neighboring pixel's vegetation when making costly land management decisions that  
445 would potentially relocate East African populations of people, livestock and crops. The motivation of this paper  
446 stems from the opportunity to optimize the pixel assignments based on neighboring pixel data, rather than using  
447 blocks in an arbitrary grid fashion, prior to using statistical methodologies to detect vegetation changes over regions  
448 in East Africa. Knowing information about the homogeneous cluster to which a particular pixel belongs can provide  
449 valuable insights and improved methodologies.

450 Although we demonstrated our methodology using NDVI data, the procedure can be used for any spatial-temporal  
451 data, even on finer scales. Overall, by using dynamic programming to formulate a multidimensional temporal  
452 assignment problem implemented by the heuristic procedure, we were able to reassign pixels to adjacent clusters  
453 based on similar NDVI values over time. The results of this analysis create more homogeneous regions of East  
454 Africa for decision makers to draw inferences regarding vegetation changes. We have demonstrated a powerful tool  
455 for homogeneous cluster creation of pixels undergoing land-cover change using temporal satellite data.

456 Efficient land use for economic sustainability and effective land use for environmental sustainability have become  
457 very important topics addressed by Cole, Et al. (2000) and Duveiller, Et al. (2007). This research may be directly  
458 extended to consider additional characteristics of land and identify appropriate land use as in Usongo & Nagahuedi  
459 (2008). This is especially important when considering the inclusion of multiple land purposes: residential, farm,  
460 riparian borders, industrial, commercial, etc.

461 Another avenue to explore in future research is to extend the proposed methodologies to other applications of spatio-  
462 temporal data. For example, monitoring and detecting transient sources in the night sky, specifically Type Ia  
463 supernovae transients, is an area of astronomical research that receives much attention. Spatio-temporal astronomy  
464 data has spatial dependencies that exist between pixels in astronomical images, which is well suited for a  
465 multidimensional temporal reassignment to create homogenous clusters.

466 With extension of this work to other special problems, finding optimal weights will become important and relevant  
467 work. Though the pixel assignment problems ultimately unveiled the appropriate weights through an iterative  
468 approach, problems with extended criteria provide a greater challenge in determining appropriate or optimal  
469 weights. We anticipate determination of optimal weights to be evaluated as future research as well.



470 **Appendix A**

471 **Proof.** We prove that the mdFDR is controlled at desired level  $\alpha$ , by borrowing some ideas in Clements, et. al.  
 472 (2014). Let  $R$  be the total number of  $H_{ij}$ 's that have been rejected, and  $V$  and  $U$ , respectively, be the numbers of  
 473 Types I and III errors that occurred out of these  $R$  rejections. Then

$$474 \quad \text{mdFDR} = \text{FDR} + \text{dFDR} = E\left(\frac{V+U}{\max\{R,1\}}\right), \quad (A1)$$

475 since  $\text{FDR} = E\left(\frac{V}{\max\{R,1\}}\right)$  and  $\text{dFDR} = E\left(\frac{U}{\max\{R,1\}}\right)$  is the directional FDR. Let us consider using  $H_{ij}$  as an indicator  
 476 variable with  $H_{ij} = 0$  (or 1), indicating that Brillinger's null hypothesis  $H_{ij}: \beta_{ij} = 0$  is true (or false). Then,

$$477 \quad V = \sum_{i=1}^m \sum_{j=1}^{n_i} I(H_{ij} = 0, P_{ij} \leq S\alpha/mn_i) \quad (A2)$$

478 where  $S$  is the number of significant subregions in the first stage of the procedure. Hence,

$$479 \quad \text{FDR} = E\left(\frac{V}{\max\{R,1\}}\right) \quad (A3)$$

$$480 \quad = \sum_{i=1}^m \sum_{j=1}^{n_i} E\left(\frac{I(H_{ij} = 0, P_{ij} \leq S\alpha/mn_i)}{\max\{R,1\}}\right) \quad (A4)$$

$$481 \quad \leq \sum_{i=1}^m \sum_{j=1}^{n_i} I(H_{ij} = 0) E\left(\frac{I\left(P_{ij} \leq \frac{S\alpha}{mn_i}\right)}{\max\{S,1\}}\right) \quad (A5)$$

482 since  $R \geq S$  [borrowing the idea from Guo and Sarkar (2012)]. Let  $S^{(-i)}$  be the number of significant subregions that  
 483 would have been obtained if we had completely ignored the  $i^{\text{th}}$  subregion and applied the first-stage BH method to  
 484 the rest of the  $m - 1$  subregion  $p$ -values using the critical values  $\frac{i\alpha}{m}, i = 2, 3, \dots, m$ . Then, it can be shown that

$$485 \quad \frac{I\left(P_{ij} \leq S\alpha/mn_i\right)}{\max\{S,1\}} = \sum_{s=1}^m \frac{I\left(P_{ij} \leq \frac{s\alpha}{mn_i}, S = s\right)}{s} \quad (A6)$$

$$486 \quad = \sum_{s=1}^m \frac{I\left(P_{ij} \leq \frac{s\alpha}{mn_i}, S^{(-i)} = s - 1\right)}{s} \quad (A7)$$

487 Since we assume the  $m$  subregions are independent, taking expectation and inserting into FDR definition gives us



488 
$$\text{FDR} \leq \sum_{i=1}^m \sum_{j=1}^{n_i} I(H_{ij} = 0) \sum_{s=1}^m \frac{1}{s} \frac{s\alpha}{mn_i} \Pr(S^{(-i)} = s - 1) \quad (\text{A8})$$

489 
$$= \alpha \sum_{i=1}^m \frac{1}{mn_i} \sum_{j=1}^{n_i} I(H_{ij} = 0) \quad (\text{A9})$$

490 
$$= \frac{\alpha}{m} \sum_{i=1}^m \pi_{i0} \quad (\text{A10})$$

491 where  $\pi_{i0}$  is the proportion of true null hypotheses among the total  $n_i$  null hypotheses in the  $i^{\text{th}}$  subregion.

492

493 We now work with the dFDR. Let  $\delta_{ij} = \text{sign}(\beta_{ij})$  representing the true sign of the Brillinger's monotonic trend  
 494 parameter  $\beta_{ij}$   $j^{\text{th}}$  location in the  $i^{\text{th}}$  subregion and  $T_{ij}$  is the test statistic. Now,  $U$  can be expressed as follows:

495 
$$U = \sum_{i=1}^m \sum_{j=1}^{n_i} I\left(H_{ij} = 1, P_{ij} \leq \frac{S\alpha}{mn_i}, T_{ij}\delta_{ij} < 0\right) \quad (\text{A11})$$

496 from which we first have

497

498 
$$\text{dFDR} = E\left(\frac{U}{\max\{R, 1\}}\right) \quad (\text{A12})$$

499 
$$U = \sum_{i=1}^m \sum_{j=1}^{n_i} I(H_{ij} = 1) E\left(\frac{I\left(P_{ij} \leq \frac{S\alpha}{mn_i}, T_{ij}\delta_{ij} < 0\right)}{\max\{R, 1\}}\right) \quad (\text{A13})$$

500 Making arguments similar to those used for the FDR, we then have

501 
$$\text{dFDR} \leq \sum_{i=1}^m \sum_{j=1}^{n_i} I(H_{ij} = 1) \sum_{s=1}^m \frac{1}{s} \Pr\left(P_{ij} \leq \frac{s\alpha}{mn_i}, T_{ij}\delta_{ij} < 0\right) \Pr(S^{(-i)} = s - 1) \quad (\text{A14})$$

502 Notice that  $P_{ij} = 2[1 - \Phi(|T_{ij}|)]$ , where  $\Phi$  is the cumulative distribution function of the standard normal.

503 Therefore, assuming without any loss of generality that  $\beta_{ij} > 0$  when  $H_{ij} = 1$ , we have, for such  $H_{ij}$ ,

504 
$$\Pr\left(P_{ij} \leq \frac{s\alpha}{mn_i}, T_{ij}\delta_{ij} < 0\right) \quad (\text{A15})$$



$$505 \quad = \Pr_{\beta_{ij}>0} \left( |T_{ij}| \geq F^{-1} \left( 1 - \frac{s\alpha}{2mn_i} \right), T_{ij} < 0 \right) \quad (A16)$$

$$506 \quad = \Pr_{\beta_{ij}>0} \left( T_{ij} \leq -F^{-1} \left( 1 - \frac{s\alpha}{2mn_i} \right) \right) \quad (A17)$$

$$507 \quad \leq \Pr_{\beta_{ij}=0} \left( T_{ij} \leq -F^{-1} \left( 1 - \frac{s\alpha}{2mn_i} \right) \right) \quad (A18)$$

$$508 \quad = \frac{s\alpha}{2mn_i}.$$

509 The last inequality follows from the fact that, when  $H_{ij}=1$ , the distribution of  $T_{ij}$  is stochastically increasing in  $\beta_{ij}$ .

510 Continuing, we have

$$511 \quad \text{dFDR} \leq \frac{\alpha}{2m} \sum_{i=1}^m \frac{1}{n_i} \sum_{j=1}^{n_i} I(H_{ij} = 1) = \frac{\alpha}{2m} \sum_{i=1}^m \pi_{i1} \quad (A19)$$

512

513 where  $\pi_{i1}$  is the proportion of false null hypotheses among the total  $n_i$  null hypotheses in the  $i^{\text{th}}$  subregion. Thus, we

514 combine and finally prove the desired result.

$$515 \quad \text{mdFDR} \leq \frac{\alpha}{m} \sum_{i=1}^m \left( \pi_{i0} + \frac{1}{2} \pi_{i1} \right) = \frac{\alpha}{m} \sum_{i=1}^m \left( \frac{1 + \pi_{i0}}{2} \right) \quad (A20)$$

516



517 **Author Contribution**

518 Nicolle Clements completed all multiple testing evaluation and statistical analysis. Virginia Miori completed all  
519 decision model development. Virginia Miori developed the heuristic approach; the heuristic was refined by  
520 Virginia Miori and Nicolle Clements. The development of computer code to implement the heuristic was completed  
521 by Brian Segulin.

522 **Competing Interests**

523 The authors declare that they have no conflict of interest.

524 **Acknowledgements**

525 The NDVI data set was collected as part of a Michigan State University research project, namely, the “Dynamic  
526 Interactions among People, Livestock, and Savanna Ecosystems under Climate Change” project (funded by the  
527 National Science Foundation Biocomplexity of Coupled Human and Natural Systems Program, Award No.  
528 BCS/CNH 0709671).

529



530 **References**

- 531 Balas, E. and Saltman, M.J.: An algorithm for the three-index assignment problem, *Oper. Res.*, 39(1), 150–161,  
532 1991.
- 533 Bandelt, H.J., Cramab, Y., and Spieksma, F.C.R.: Approximation algorithms for multi-dimensional assignment  
534 problems with decomposable costs, *Discrete Applied Mathematics*, 49, 20–25, 1994.
- 535 Bandelt, H.J., Maas, A., and Spieksma, F.C.R.: Local search heuristics for multi-index assignment problems with  
536 decomposable costs, *The Journal of the Operational Research Society*, 55(7), 694–704, 2004.
- 537 Brillinger, D.R.: Consistent detection of a monotonic trend superposed on a stationary time series, *Biometrika*, 76,  
538 23–30, 1989.
- 539 Benjamini, Y. and Hochberg, Y.: Controlling the false discovery rate: A practical and powerful approach to multiple  
540 testing, *Journal of the Royal Statistical Society*, 57, 289–300, 1995.
- 541 Benjamini, Y., Krieger, K., and Yekutieli, D.: Adaptive linear step-up procedures that control the false discovery  
542 rate, *Biometrika*, 93, 491–507, 2006.
- 543 Benjamini, Y. and Yekutieli, D.: The control of the false discovery rate in multiple testing under dependency,  
544 *Annals of Statistics*, 29, 1165–1188, 2001.
- 545 Benjamini, Y. and Yekutieli, D.: False discovery rate-adjusted multiple confidence intervals for selected parameters,  
546 *Journal of the American Statistical Association*, 100, 71–93, 2005.
- 547 Blanchard, G. and Roquain, E.: Adaptive FDR control under independence and dependence. *Journal of Machine  
548 Learning Research*, 10, 2837–2871, 2009.
- 549 Cao, K., Batty, M., Huang, B., Liu, Y., and Chen, J.: Spatial multi-objective land use optimization: extensions to the  
550 non-dominated sorting genetic algorithm-II, *International Journal of Geographical Information Science*, 25(12),  
551 1949–1969, 2011.
- 552 Cao, K., Huang, B., Wang, S., and Lin, H.: Sustainable land use optimization using boundary-based fast genetic  
553 algorithm, *Computers, Environment and Urban Systems*, 36, 257–269, 2012.
- 554 Chen, J., Jonsson, P., and Tamura, M.: A simple method for reconstructing a high-quality NDVI time-series data set  
555 based on the Savitzky–Golay filter, *Remote Sensing of Environment*, 91, 332–344, 2004.
- 556 Clements, N., Sarkar, S., Zhao, Z., and Kim, D.: Applying multiple testing procedures detect changes in East  
557 African vegetation, *Annals of Applied Statistics*, 8(1), 286–308, 2014.
- 558 Cole, J.E., Dunbar, R.B., McClanahan, T.R., and Muthiga, N.A.: Tropical pacific forcing of decadal SST variability  
559 in the western Indian Ocean over the past two centuries, *Science*, 287, 617–619, 2000.
- 560 Cressie, N. and Wikle, C.K.: *Statistics for spatio-temporal data*, Wiley, Hoboken (NJ), 2011.
- 561 Curran, P.J.: Multispectral remote sensing of vegetation amount, *Progress in Physical Geography*, 4, 315–341, 1980.
- 562 Duveiller, G., DeFourmy, P., Desclee, B., and Mayaux, P.: Deforestation in Central Africa: Estimates at regional,  
563 national and landscape levels by advanced processing of systematically-disturbed Landsat extracts, *Remote Sensing  
564 of Environment*, 112, 1969–1981, 2007.
- 565 Foody, G.M.: Geographical weighting as a further refinement to regression modeling: An example focused on the  
566 NDVI–rainfall relationship, *Remote Sensing of Environment*, 88, 283–293, 2003.



- 567 Franz, L.S. and Miller, J.L.: Scheduling medical residents to rotations: Solving the large-scale multiperiod staff  
568 assignment problem, *Oper. Res.*, 41(2), 269–279, 1993.
- 569 Frieze, A.M. and Yadegar, J.: An algorithm for solving 3-dimensional assignment problems with application to  
570 scheduling a teaching practice, *The Journal of the Operational Research Society*, 32(11), 989–995, 1981.
- 571 Gasson, R.: Goals and values of farmers, *Journal of Agricultural Economics*, 24(3), 521–537, 1973.
- 572 Gilbert, K.C. and Hofstra, R.B.: Multidimensional assignment problems, *Decision Sciences*, 19(2), 306–321, 1988.
- 573 Guo, W., Sarkar, S. and Peddada, S.: Controlling false discoveries in multidimensional directional decisions, with  
574 applications to gene expression data on ordered categories, *Biometrics*, 66, 485–492, 2009.
- 575 Gutin, G., Goldengorin, B. and Huang, J.: Worst case analysis of max-regret, greedy and other heuristics for  
576 multidimensional assignment and traveling salesman problems, *Journal of Heuristics*, 14, 169–181, 2008.
- 577 Harper, W.H. and Eastman, C.E.: An evaluation of goal hierarchies for small farm operators, *American Journal of*  
578 *Agricultural Economics*, 62(4), 742–747, 1980.
- 579 Hayashi, K.: Multicriteria analysis for agricultural resource management: A critical survey and future perspectives,  
580 *European Journal of Operational Research*, 122(2), 486–500, 2000.
- 581 Hayes, D.J. and Sader, S.A.: Comparison of change-detection techniques for monitoring tropical forest clearing and  
582 vegetation regrowth in a time series, *Photogrammetric Engineering and Remote Sensing*, 67, 1067–1075, 2001.
- 583 Hochberg, Y. and Tamhane, A.: *Multiple comparison procedures*. New York, New York: Wiley, 1987.
- 584 Hochberg, Y.: A sharper bonferroni procedure for multiple tests of significance, *Biometrika*, 75, 800–802, 1988.
- 585 Holland, B.S. and Copenhaver, M.D.: An improved sequentially rejective bonferroni test procedure, *Biometrics*, 43,  
586 417–423, 1987.
- 587 Holm, S.: A simple sequential rejective multiple test procedure, *Scandinavian Journal of Statistics*, 6, 65–70, 1979.
- 588 Jackson, R.D., Slater, P.N., and Pinter, P.J.: Discrimination of growth and water stress in wheat by various  
589 vegetation indices through clear and turbid atmospheres, *Remote Sensing of Environment*, 13, 187–208, 1983.
- 590 Karapetyan, D. and Gutin, G.: Local search heuristics for the multidimensional assignment problem, *Journal of*  
591 *Heuristics*, 17, 201–249, 2011.
- 592 Krokmal, P.A., Grundel, D.A., and Pardalos, P.M.: Asymptotic behavior of the expected optimal value of the  
593 multidimensional assignment problem, *Mathematical Programming B*, 109, 525–551, 2007.
- 594 Kuchma, T., Tarariko, O., and Syrotenko, O.: Landscape diversity indexes application for agricultural land use  
595 optimization, 6th International Conference on Information and Communication Technologies in Agriculture, Food  
596 and Environment, *Procedia Technology*, 8, 566 – 569, 2013.
- 597 Kutcher, G.P. and Norton, R.D.: Operations research methods in agricultural policy analysis, *European Journal of*  
598 *Operational Research*, 10(4), 333–345, 1982.
- 599 Kuroki, Y. and Matsui, T.: Approximation algorithm for multidimensional assignment problem minimizing the sum  
600 of squared errors, *Mathematical Engineering Technical Reports* 03, 2007.
- 601 Liu, Y., Peng, J., Jiao, L., and Liu, Y.: A heuristic land-use allocation model using patch-level operations and  
602 knowledge-informed rules, *PLoS ONE*, 11(6), 2016.



- 603 Memarian, H., Balasundram, S.K., Abbaspour, K.C., Talib, J.B., Sung, T.B., and Alias, M.S.: Integration of analytic  
604 hierarchy process and weighted goal programming for land use optimization at the watershed scale, Turkish Journal  
605 of Engineering & Environmental Sciences, 38, 139-158, 2014.
- 606 Miori, V.M.: A dynamic programming approach to the stochastic truckload routing problem, The Supply Chain in  
607 Manufacturing, Distribution and Transportation: Modeling, Optimization and Applications, CRC Press, 179-203,  
608 2008.
- 609 Miori, V.M.: A multiple objective goal programming approach to the truckload routing problem, Journal of the  
610 Operational Research Society, 62, 1524-1532, 2011.
- 611 Miori, V.M.: The pollyanna problem: assignment of participants in a gift exchange, International Journal of  
612 Business Intelligence Research, 5(1), 1-12, 2014.
- 613 Norton, R.D. and Scandizzo, P.L.: Market equilibrium computations in activity analysis models, Oper. Res., 29(2),  
614 243-262, 1981.
- 615 OCHA: Eastern Africa drought humanitarian report No. 3, UN Office for the Coordination of Humanitarian Affairs,  
616 2011.
- 617 Önal, H. and McCarl, B.: Aggregation of heterogeneous firms in mathematical programming models, European  
618 Review of Agricultural Economics, 16(4), 499-513, 1989.
- 619 Phillips, N.V.: A weighting function for pre-emptive multicriteria assignment problems, The Journal of the  
620 Operational Research Society, 38(9), 787-802, 1987.
- 621 Pierskalla, W.P.: The multidimensional assignment problem, Oper. Res, 16(2), 422-431, 1968.
- 622 Poore, A.B. and Rijavec, N.: A lagrangian relaxation algorithm for multidimensional assignment problems arising  
623 from multitarget tracking, SIAM Journal on Optimization, 3(3), 544-563, 1993.
- 624 Robertson, A.J.: A set of greedy randomized adaptive local search procedure (GRASP) implementations for the  
625 multidimensional assignment problem, Computational Optimization and Applications, 19(2), 145-164, 2001.
- 626 Romero, C. and Rehman, T.: Multiple criteria analysis for agricultural decisions, Elsevier, Amsterdam, The  
627 Netherlands (original publication (1989), 2003.
- 628 Sadeghi, S.H.R., Jalili, K., and Nikkani, D. (2009). Land use optimization in watershed scale, Land Use Policy, 26,  
629 186-193.
- 630 Sahebgharani, A.: Multi-objective land use optimization through parallel particle SWARM Algorithm: Case study  
631 Baboldasht district of Isfahah, Iran, Journal of Urban and Environmental Engineering, 10(1), 42-49, 2016.
- 632 Samuelson, P.A.: Spatial price equilibrium and linear programming, American Economic Review, 42(2), 283-303,  
633 1952.
- 634 Sarkar, S.K.: Some probability inequalities for ordered MTP2 random variables: a proof of the Simes conjecture,  
635 Annals of Statistics, 26, 494-504, 1998.
- 636 Sarkar, S. K.: Some results on false discovery rate in stepwise multiple testing procedures, Annals of Statistics, 30,  
637 239-257, 2002.
- 638 Sarkar, S. K.: Generalizing Simes' test and Hochberg's stepup procedure, Annals of Statistics, 36(1), 337-363,  
639 2008.



- 640 Sarkar, S.K. and Chang, C.K.: The Simes method for multiple hypothesis testing with positively dependent test  
641 statistics, *Journal of the American Statistical Association*, 92, 1601-1608, 1997.
- 642 Sarkar, S. and Zhou, T.: Controlling Bayes directional false discovery rate in random effects model, *Journal of*  
643 *Statistical Planning and Inference*, 138, 682–693, 2008.
- 644 Shaffer, J.: Multiplicity, directional type III errors, and the null hypothesis, *Psychological Methods*, 7, 356369,  
645 2002.
- 646 Šidák, Z. K.: Rectangular confidence regions for the means of multivariate normal distributions, *Journal of the*  
647 *American Statistical Association*, 62 (318), 626–633, 1967.
- 648 Stewart, T.J., Janssen, R., and van Herwijnen, M.: A genetic algorithm approach to multiobjective landuse planning,  
649 *Computers & Operations Research*, 31, 2293–2313, 2004.
- 650 Storey, J., Taylor, J. and Siegmund, D.: Strong control, conservative point estimation and simultaneous conservative  
651 consistency of false discovery rates: a unified approach, *Journal of the Royal Statistical Society, B*, 66, 187–205,  
652 2004.
- 653 Sunandar, A.D., Suhendang, E., Hendrayanto, Surati Jaya, I.N., Marimin.: Land use optimization in Asahan  
654 Watershed with linear programming and SWAT model, *International Journal of Sciences: Basic and Applied*  
655 *Research*, 18(1), 63-78, 2014.
- 656 Takayama, T. and Judge, G.G.: Spatial equilibrium and quadratic programming, *Journal of Farm Economics*, 46(1),  
657 67–93, 1964.
- 658 Truong, V.A. and Roundy, R.O.: Multidimensional approximation algorithms for capacity-expansion problems,  
659 *Oper. Res.*, 59(2), 313-327, 2011.
- 660 Tucker, C., Pinzon, J., Brown, M., Slayback, D., Pak, E., Mahoney, R., Vermote, E. and Saleous, N.: An extended  
661 AVHRR 8-km NDVI data set compatible with MODIS and SPOT vegetation NDVI data, *International Journal of*  
662 *Remote Sensing*, 26, 4485–4498, 2005.
- 663 Usongo, L. and Nagahuedi, J.: Participatory land-use planning for priority landscapes of the Congo Basin, *Unasylva*,  
664 230, 17–24, 2008.
- 665 Vrieling, A., De Beurs, K.M., and Brown, M.E.: Recent trends in agricultural production of Africa based on  
666 AVHRR NDVI time series, *Proceedings of the SPIE Conference: Remote Sensing for Agriculture, Ecosystems and*  
667 *Hydrology X*, 2008.
- 668 Wang, C.H. and Guldmann, J.M.: A land-use allocation optimization model to mitigate potential seismic damages,  
669 *Environment and Planning B: Planning and Design*, 42, 730 – 753, 2015.
- 670 Weintraub, A. and Romero, C.: Operations research models and the management of agriculture and forestry  
671 resources: A review and comparison, *Interfaces*, 36(5), 446-457, 2017.
- 672 Wheeler, B.M. and Russell, J.R.M.: Goal programming and agricultural planning, *Oper. Res. Quart*, 28(1), 21–32,  
673 1977.
- 674 White, D.J.: A special multi-objective assignment problem, *The Journal of the Oper. Res. Society*, 35(8), 759–767,  
675 1984.
- 676 Williams, V., Jones, L., and Tukey, J.: Controlling error in multiple comparisons, with examples from state-to-state  
677 differences in educational achievement, *Journal of Educational and Behavioral Statistics*, 24, 42–69, 1999.